

Active RC Single-Opamp Design of Driving-Point Impedances

PETER HORN, MEMBER, IEEE, AND GEORGE S. MOSCHYTZ, FELLOW, IEEE

Abstract—The active RC simulation of LC filters is of interest, due to the excellent sensitivity properties thereby obtained. Most known designs of active RC driving-point impedances necessary for the simulation of an LC filter, require two opamps per impedance. In this paper a method is presented that realizes general second-order driving-point impedances with only one opamp and with a minimum number of capacitors and resistors. The method is based upon an interesting property of active RC driving-point impedances which is derived in the paper. This property relates the well-known properties of driving-point impedance poles and zeros to the zeros of the feedback voltage-transfer functions in a single-opamp second-order filter structure.

I. INTRODUCTION

THE LOW SENSITIVITY in the passband of passive LC filters [1] is the reason for numerous investigations [2]–[6] into the design of active filters based on LC structures. Recently, several papers [7]–[10], [16] have been published describing the active RC simulation of first- or second-order LCR impedances using only one opamp. This paper is an additional contribution to this theme. It deals with the design of general active RC driving-point impedances of arbitrary order using networks that contain only one opamp. The design method is based on a useful property of the active RC driving-point impedance of a network in which a single opamp is used in the differential input mode. In order to derive this property and the design method itself, it is necessary to review an analysis procedure of the network that is based on signal-flow graph theory. This is described in the following section.

II. THE SIGNAL-FLOW GRAPH ANALYSIS OF TRANSFER- AND DRIVING-POINT FUNCTIONS OF GENERAL SINGLE-OPAMP ACTIVE RC NETWORKS

A. Voltage Transfer Functions

Consider the general active network shown in Fig. 1. It comprises a five-terminal RC network N and a differential-input opamp with open-loop gain A . Letting $V_d = V_k - V_l$, and using the principle of superposition with respect to the voltage sources V_i and V_m , the signal-flow graph of Fig. 2 is obtained. The transfer functions t_{id} and t_{md} are associated with the passive RC network N and are obtained from the definite admittance matrix [11] of N ,

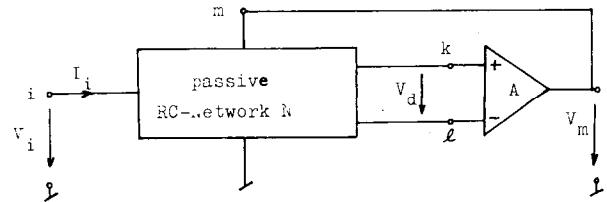


Fig. 1. General single-opamp active network.

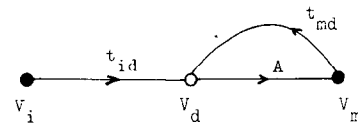


Fig. 2. Signal-flow graph of network in Fig. 1.

namely

$$[y] = \begin{bmatrix} 1 & 2 & \cdots & i & \cdots & k & l & m & \cdots \\ 1 & y_{11} & y_{12} & \cdots & y_{1i} & \cdots & y_{1k} & y_{1l} & y_{1m} & \cdots \\ 2 & y_{21} & \cdot & \cdot & \cdot & \cdot & \cdot & \cdot & \cdot & \cdots \\ \vdots & \cdot & \cdot & \cdot & \cdot & \cdot & \cdot & \cdot & \cdot & \cdots \\ \vdots & \cdot & \cdot & \cdot & \cdot & \cdot & \cdot & \cdot & \cdot & \cdots \\ i & y_{i1} & \cdot & \cdots & y_{ii} & \cdots & y_{ik} & y_{il} & y_{im} & \cdots \\ \vdots & \cdot & \cdot & \cdot & \cdot & \cdot & \cdot & \cdot & \cdot & \cdots \\ k & \cdot & \cdot & \cdot & \cdot & \cdot & \cdot & \cdot & \cdot & \cdots \\ l & y_{l1} & \cdot & \cdots & y_{li} & \cdots & y_{lk} & y_{ll} & y_{lm} & \cdots \\ m & y_{m1} & \cdot & \cdots & y_{mi} & \cdots & y_{mk} & y_{ml} & y_{mm} & \cdots \\ \vdots & \cdot & \cdot & \cdot & \cdot & \cdot & \cdot & \cdot & \cdot & \cdots \\ \vdots & \cdot & \cdot & \cdot & \cdot & \cdot & \cdot & \cdot & \cdot & \cdots \end{bmatrix} \quad (1)$$

From (1) the forward transfer function t_{id} results as

$$t_{id} = \frac{n_{id}}{\hat{d}} = \frac{V_k - V_l}{V_i} \bigg|_{V_m=0} = \frac{\Delta_{km}^{im} - \Delta_{lm}^{im}}{\Delta_{im}^{im}} \quad (2)$$

and the feedback transfer function t_{mdis} as

$$t_{mdis} = \frac{n_{mdis}}{\hat{d}} = \frac{V_k - V_l}{V_m} \bigg|_{V_i=0} = \frac{\Delta_{ik}^{im} - \Delta_{il}^{im}}{\Delta_{im}^{im}} \quad (3)$$

where Δ_{cd}^{ab} is a second cofactor of $[y]$. It is obtained by deleting rows a and b , and columns c and d from $[y]$ and multiplying the resulting minor by $(-1)^{a+b+c+d}$. The subscripts i and s in t_{mdis} indicate that the feedback function t_{md} is obtained with the input terminal i shorted to ground (see Fig. 4(b)).

Manuscript received January 11, 1978. This work was supported by Standard Telephone and Radio Ltd., Zurich, Switzerland.

The authors are with the Institute of Telecommunications, Swiss Federal Institute of Technology, Zurich, Switzerland.

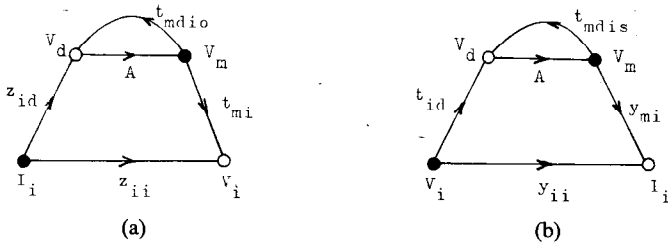


Fig. 3. Driving-point impedance (a), and admittance (b), signal-flow graphs for network in Fig. 1.

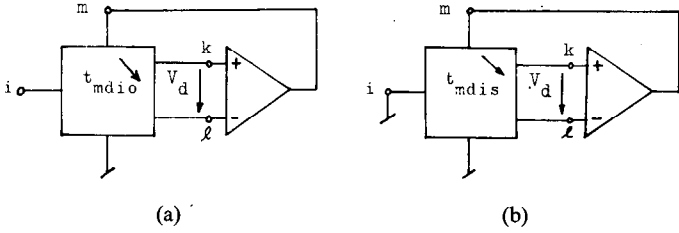


Fig. 4. Network of Fig. 1 with corresponding feedback functions. Driving terminal open (a), shorted (b).

From Fig. 2 the overall voltage transfer function T_{im} results as

$$T_{im} = \frac{V_m}{V_i} = \frac{At_{id}}{1 - At_{mdis}} \Big|_{A \rightarrow \infty} = -\frac{n_{id}}{n_{mdis}} = -\frac{\Delta_{km}^{im} - \Delta_{lm}^{im}}{\Delta_{ik}^{im} - \Delta_{il}^{im}} \quad (4)$$

Thus the zeros of T_{im} are the zeros of the forward transfer function t_{id} , the poles of T_{im} are the zeros of the feedback transfer function t_{mdis} . This property has been used to find all possible zeros of a voltage transfer function obtainable with a given active network topology [12].

B. Driving-Point Functions

The driving-point impedance of the network in Fig. 1 can be obtained in one of two ways. First, the network can be driven from a current source (sometimes referred to as a soldering-type entry [19], [20]) and the resulting input voltage then established. This corresponds to the signal-flow graph in Fig. 3(a). The driving-point impedance is then

$$Z_i = \frac{V_i}{I_i} = z_{ii} + \frac{A \cdot z_{id} t_{mi}}{1 - At_{mdio}} \Big|_{A \rightarrow \infty} = z_{ii} - \frac{t_{mi}}{t_{mdio}} z_{id} \quad (5)$$

where the subscripts i and o in t_{mdio} imply that the input terminal i is open (see Fig. 4(a)).

The second method is to drive the network from a voltage source (sometimes referred to as a pliers-type entry [19], [20]) and to determine the input current. This corresponds to the signal-flow graph in Fig. 3(b). The resulting driving-point admittance is

$$Y_i = \frac{I_i}{V_i} = y_{ii} + \frac{At_{id} y_{mi}}{1 - At_{mdis}} \Big|_{A \rightarrow \infty} = y_{ii} - \frac{t_{id}}{t_{mdis}} y_{mi} \quad (6)$$

Using Cramer's rule, the immittance and transfer functions required for the evaluation of (5) and (6) can be directly obtained from $[y]$ in (1). The resulting expressions, given in terms of the corresponding cofactors are listed in Table I. Note that t_{mdio} and t_{mdis} are the feedback transfer functions for the case that the input terminal i is open (i.e., driven from a current source) and shorted (i.e., driven from a voltage source), respectively. This distinction is not generally made in the computation of transfer functions since the *voltage* transfer function (i.e., driven from a voltage source) is usually of interest. Thus the function t_{md} occurring in connection with a transfer function is generally t_{mdis} .

Naturally, the driving-point functions can be obtained more easily using established methods such as that of Nathan [11]. However, the expressions obtained here are necessary in order to derive a useful property of driving-point impedances that is valid for any structure resembling that given in Fig. 1. This property is described in what follows.

III. THE DRIVING-POINT IMPEDANCE OF ACTIVE RC-NETWORKS COMPRISING A SINGLE OPAMP

The Blackman impedance relation [13], [11] is given as follows:

$$\frac{Z_i}{Z_i(x=0)} = \frac{F_x(\text{with input terminals shorted})}{F_x(\text{with input terminals open})} \quad (7)^1$$

It states that the ratio of the driving-point impedance of a network with and without feedback (i.e., with $x \neq 0$ and $x=0$, respectively) is equal to the ratio of the return difference with respect to the feedback element x when the input terminal i is shorted and open, respectively. Applying this relation to the signal-flow graphs in Fig. 3, we obtain

$$\frac{Z_i}{z_{ii}} = \frac{F_A(V_i=0)}{F_A(I_i=0)} = \frac{1 - At_{mdis}}{1 - At_{mdio}} \Big|_{A \rightarrow \infty} = \frac{t_{mdis}}{t_{mdio}} \quad (8)$$

An equivalent expression is obtained for Y_i/y_{ii} . From Table I we have

$$t_{mdis} = \frac{V_d}{V_m} \Big|_{V_i=0} = \frac{n_{mdis}}{d_{mdis}} = \frac{\Delta_{ik}^{im} - \Delta_{il}^{im}}{\Delta_{im}^{im}} \quad (9a)$$

$$t_{mdio} = \frac{V_d}{V_m} \Big|_{I_i=0} = \frac{n_{mdio}}{d_{mdio}} = \frac{\Delta_k^m - \Delta_l^m}{\Delta_m^m} \quad (9b)$$

¹In the present discussion the input terminals will refer to the input terminal i and ground.

TABLE I
FORMULAS FOR THE CALCULATION OF THE TRANSFER FUNCTIONS
IN FIG. 3

	Driving-point impedance (Fig. 3a)	Driving-point admittance (Fig. 3b)
1	$z_{ii} = \frac{V_i}{I_i} \Big _{V_m=0} = \frac{\Delta_{im}^{im}}{\Delta_m^m}$	$y_{ii} = \frac{I_i}{V_i} \Big _{V_m=0} = \frac{\Delta_m^m}{\Delta_{im}^{im}}$
2	$z_{id} = \frac{V_k - V_t}{I_i} \Big _{V_m=0} = \frac{\Delta_{km}^{im} - \Delta_{tm}^{im}}{\Delta_m^m}$	$t_{id} = \frac{V_k - V_t}{V_i} \Big _{V_m=0} = \frac{\Delta_{km}^{im} - \Delta_{tm}^{im}}{\Delta_{im}^{im}}$
3	$t_{mdio} = \frac{V_k - V_t}{V_m} \Big _{I_i=0} = \frac{\Delta_m^m - \Delta_{tm}^m}{\Delta_m^m}$	$t_{mdis} = \frac{V_k - V_t}{V_m} \Big _{V_i=0} = \frac{\Delta_{ik}^{im} - \Delta_{it}^{im}}{\Delta_{im}^{im}}$
4	$t_{mi} = \frac{V_i}{V_m} \Big _{I_i=0} = \frac{\Delta_m^m}{\Delta_m^m}$	$y_{mi} = \frac{I_i}{V_m} \Big _{V_i=0} = -\frac{\Delta_{im}^{im}}{\Delta_{im}^{im}}$
5	$Z_i = z_{ii} + \frac{\Delta z_{id} t_{mi}}{1 - \Delta t_{mdio}} \Big _{A \rightarrow \infty} = \frac{\Delta_{im}^{im}}{\Delta_m^m} - \frac{\Delta_{km}^{im} - \Delta_{tm}^{im}}{\Delta_m^m} \cdot \frac{\Delta_{im}^{im}}{\Delta_{im}^{im}}$	$Y_i = y_{ii} + \frac{\Delta t_{id} y_{mi}}{1 - \Delta t_{mdis}} \Big _{A \rightarrow \infty} = \frac{\Delta_m^m}{\Delta_{im}^{im}} + \frac{\Delta_{km}^{im} - \Delta_{tm}^{im}}{\Delta_{im}^{im}} \cdot \frac{\Delta_{im}^{im}}{\Delta_{im}^{im}}$

Thus with (8) and impedance formula 1 of Table I we obtain

$$Z_i|_{A \rightarrow \infty} = \frac{\Delta_{ik}^{im} - \Delta_{it}^{im}}{\Delta_k^m - \Delta_t^m} = \frac{n_{mdis}}{n_{mdio}} = \frac{n_{md}(\text{driven from voltage source})}{n_{md}(\text{driven from current source})} \quad (10)$$

This expression states that the driving-point impedance at any terminal of a network of type given in Fig. 1 is determined by the zeros of the feedback transfer functions from the amplifier output to the differential input of the amplifier.

The zeros of the driving-point impedance are the zeros of the feedback function t_{md} with the driving terminal shorted (voltage source at the input); the poles of the driving-point impedance are the zeros of the feedback function t_{md} with the driving terminal open (current source at the input).

Referring to the configuration in Fig. 1, the zeros of the driving-point impedance at terminal i are the zeros of t_{mdis} (see Fig. 4(b)), the poles are the zeros of t_{mdio} (see Fig. 4(a)). This property can be used to advantage in the design of driving-point impedances using well-proven active filter structures whose voltage transfer functions are known [21]. This will be illustrated in the next section.

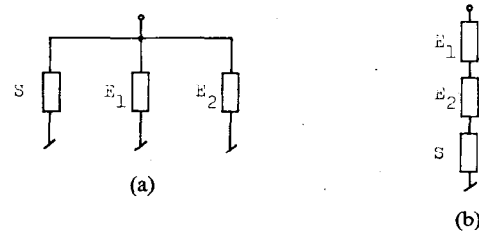


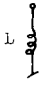
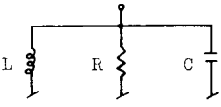
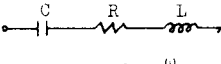
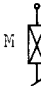
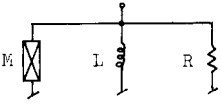
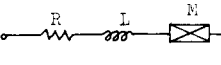
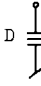
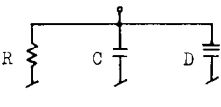
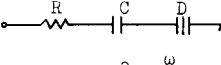
Fig. 5. Parallel and series impedance configurations.

IV. THE DESIGN OF ACTIVE RC DRIVING-POINT IMPEDANCES

A. Parallel and Series Impedance Configurations

There are two basic driving-point impedance configurations which are of particular importance in the design of simulated LC filters using active RC networks. The first corresponds to a grounded parallel combination (Fig. 5(a)), the second to a grounded series combination (Fig. 5(b)) of three elements. One of the three elements (designated S in Fig. 5) is a "simulated" element, i.e., it is an active RC network simulating a frequency-dependent component; the other two (elements E_1 and E_2 in Fig. 5) are passive, i.e., RC or RL combinations. Commonly used parallel and series impedances, and the actual compo-

TABLE II
SOME USEFUL DRIVING-POINT IMPEDANCES

Simulated Element	Parallel Configuration (Z_p) _j	Series Configuration (Z_s) _j
 $Z = sL$	 $(Z_p)_1 = R \cdot \frac{a_1 s}{s^2 + \frac{\omega_p}{q_p} s + \omega_p^2}$ $a_1 = \frac{1}{RC}, \omega_p^2 = \frac{1}{LC}, q_p = R\sqrt{\frac{C}{L}}$	 $(Z_s)_1 = R \cdot \frac{s^2 + \frac{\omega_z}{q_z} s + \omega_z^2}{b_1 s}$ $b_1 = \frac{R}{L}, \omega_z^2 = \frac{1}{LC}, q_z = \frac{1}{R} \sqrt{\frac{L}{C}}$
 $Z = s^2 M$	 $(Z_p)_2 = R \cdot \frac{a_2 s^2}{s^2 + \frac{\omega_p}{q_p} s + \omega_p^2}$ $a_2 = 1, \omega_p^2 = \frac{R}{M}, q_p = L \cdot \sqrt{\frac{1}{RM}}$	 $(Z_s)_0 = R \cdot \frac{s^2 + \frac{\omega_z}{q_z} s + \omega_z^2}{b_0}$ $b_0 = \omega_z^2 = \frac{R}{M}, q_z = \frac{\sqrt{RM}}{L}$
 $Z = \frac{1}{s^2 D}$	 $(Z_p)_0 = R \cdot \frac{a_0}{s^2 + \frac{\omega_p}{q_p} s + \omega_p^2}$ $a_0 = \omega_p^2 = \frac{1}{RD}, q_p = \frac{1}{C} \cdot \sqrt{\frac{D}{R}}$	 $(Z_s)_2 = R \cdot \frac{s^2 + \frac{\omega_z}{q_z} s + \omega_z^2}{b_2 s^2}$ $b_2 = 1, \omega_z^2 = \frac{1}{RD}, q_z = C \cdot \sqrt{\frac{R}{D}}$

nents making them up, are summarized in Table II. In both cases the impedance can be expressed in the form

$$Z = R \cdot f(s) \quad (11)$$

or, normalized with respect to the resistor R (indicated by a prime)

$$Z' = f(s) \quad (12)$$

where $f(s)$ is a dimensionless function in s . Thus the parallel configuration can be expressed by the general normalized form

$$(Z'_p)_j = \frac{a_j s^j}{s^2 + \frac{\omega_p}{q_p} s + \omega_p^2} \quad (13)$$

where j equals 0, 1, or 2, and the poles, which are defined by ω_p and q_p , are complex conjugate. Similarly the series configuration, normalized with respect to R has the general form

$$(Z'_s)_j = \frac{s^2 + \frac{\omega_z}{q_z} s + \omega_z^2}{b_j s^j} \quad (14)$$

where j equals 0, 1, or 2, and the zeros, defined by ω_z and q_z , are complex conjugate. Due to the normalization, (13) and (14) are dimensionless.

B. The Two-Step Design of Driving-Point Impedances

In order to realize the six basic driving-point impedance configurations listed in Table II, we are free to select any type of network, as long as it belongs to the category represented by Fig. 1. The selection of a suitable network should take into account such factors as circuit sensitivity to component variations and the number of components required. Furthermore, and for obvious reasons, the considerable experience accumulated in the design and development of single-amplifier building blocks providing second-order voltage transfer functions should be applicable also to the design of driving-point impedances. With this in mind, it is advisable to start out with a well proven basic active filter topology such as that shown in Fig. 6(a), (b), or (c). Note that these networks are included in the basic topology of Fig. 1. Starting out with each of these topologies, whereby resistors and capacitors are inserted as they would be in the equivalent active filter building blocks, and augmenting them along the lines discussed in

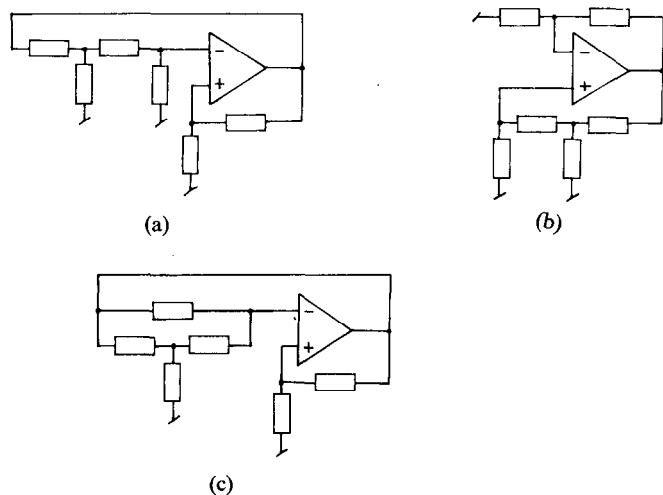


Fig. 6. Basic active filter topologies.

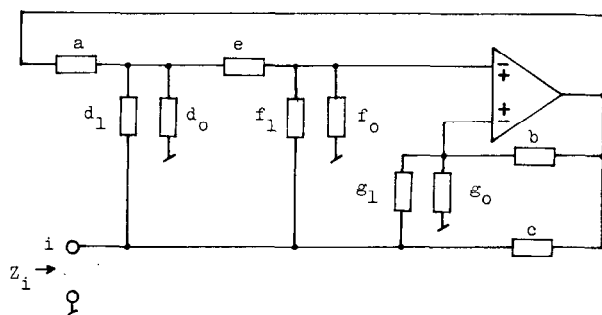


Fig. 7. Generalized active filter topology.

[21], any one of the impedance types listed in Table II can be obtained. In doing so we consider two additional design constraints, namely i) the active impedance should be canonic in terms of capacitors, i.e., only two capacitors should be used for a second-order impedance function and ii) the number of resistors should also be as low as possible.

C. A General Approach to Driving-Point Impedance Design

In the following we show how the driving-point impedance property derived in Section III can be used to design any one of the driving-point impedances listed in Table II. We start out with the generalized topology of Fig. 7 which includes the special network structures of Fig. 6. In particular the topologies of Fig. 6(a) and (b) are included here: with the upper opamp signs we have the augmented version of Fig. 6(b), with the lower signs the augmented version of Fig. 6(a). Using this generalized topology, only one analysis is necessary; any impedance in Table II can subsequently be obtained by elimination of appropriate network elements.

The analysis of the generalized impedance represented by Fig. 7 gives

$$Z_i = \frac{N(s)}{D(s)} = \frac{n_a + An_i}{d_a + Ad_i} \bigg|_{A \rightarrow \infty} = \frac{n_i}{d_i} \quad (15)$$

where

$$n_a = e(a + d_1 + d_0) \cdot (b + g_1 + g_0) + (f_1 + f_0) \cdot (a + d_1 + d_0 + e) \cdot (b + g_1 + g_0) \quad (16)$$

$$n_i = be(d_1 + d_0) + b(f_1 + f_0) \cdot (a + d_1 + d_0 + e) - ae(g_1 + g_0) \quad (17)$$

$$d_a = (b + g_0 + g_1) \{ (c + d_1 + f_1) \cdot [e(a + d_0) + f_0(a + d_0 + e)] + cf_1(a + d_1 + d_0 + e) + cd_1(e + f_0) + f_1d_1(a + d_0 + f_0) \} + (b + g_0)g_1[e(a + d_1 + d_0) + (f_1 + f_0)(a + d_1 + d_0 + e)] \quad (18)$$

$$d_i = b(c + d_1 + f_1 + g_1)[ed_0 + f_0(a + d_0 + e)] + bd_1[f_1d_0 + f_0(c + f_1 + g_1)] + g_1[ad_1f_0 + ced_0 + cf_0(a + d_1 + d_0 + e)] - g_0[ae(c + d_1 + f_1 + g_1) + cd_1e + ad_1f_1 + cf_1(a + d_1 + d_0 + e)] \quad (19)$$

Note that the polarity of the input terminals of the opamp does not influence the expression for the driving-point impedance. However, for any given impedance realization only one polarity is permissible for the opamp. It is determined by the stability of the network, and depends on the basic topology (e.g., Fig. 6(a) (b)) from which the network in question evolved.

Considering the design of the zeros of Z_i first, we can simplify $N(s)$ considerably by setting certain admittances to zero (i.e., removing them) or to infinity (i.e., shorting them). However, the number of possible realizations is still enormous, even if we take into account our two constraints i.e., i) canonic in C and ii) minimum number of resistors. With the aid of our "impedance property" discussed in Section III we can now proceed expeditiously nevertheless. Referring to Fig. 7 we assume that the input terminal of the driving-point impedance is to be driven from a voltage source. With respect to the feedback function t_{md} this implies a shorted input terminal during operation of the network, i.e., we are concerned here with t_{mdis} . In these circumstances, setting the admittance b equal to zero means that there is feedback to only one of the opamp input terminals. Then it is easy to see that a low-, high-, or bandpass feedback function t_{mdis} will provide a term a_0 , a_1s , or a_2s^2 in the numerator of Z_i . Thus we obtain a numerator associated with a parallel impedance configuration (see (13)). Using (17) and (19) it is then a simple matter to select the remaining admittance values such that the desired complex conjugate poles of Z_i are obtained. Proceeding in this manner, the parallel impedance configurations given as networks 1–10 in Table III

TABLE III
SOME PRACTICAL IMPEDANCE CONFIGURATIONS

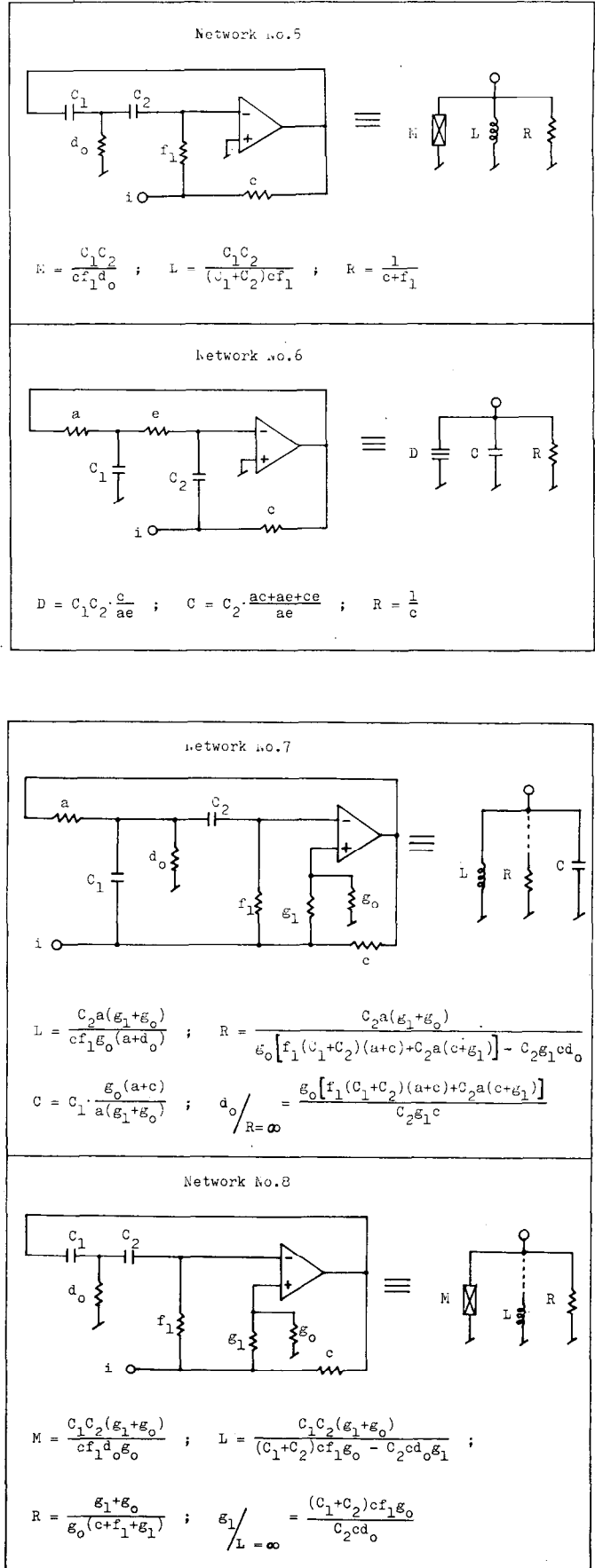
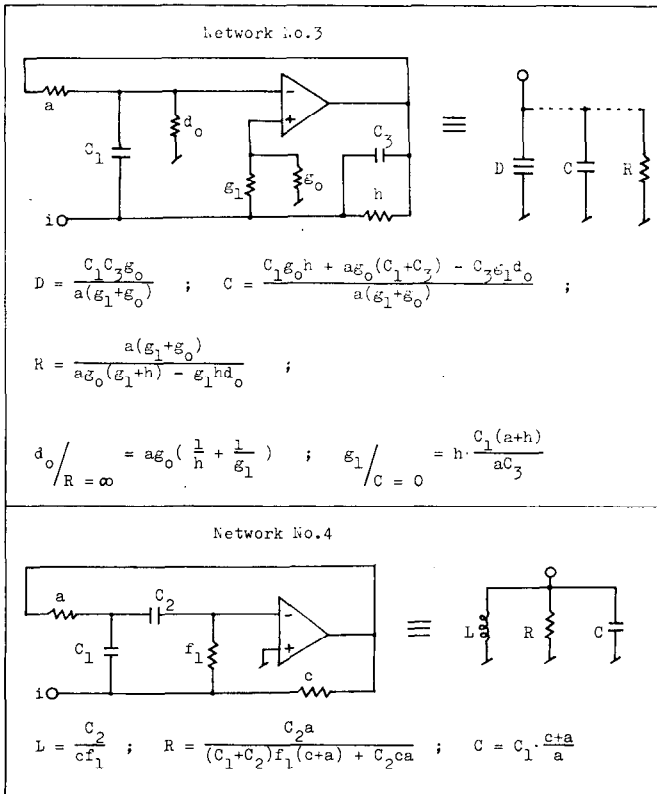
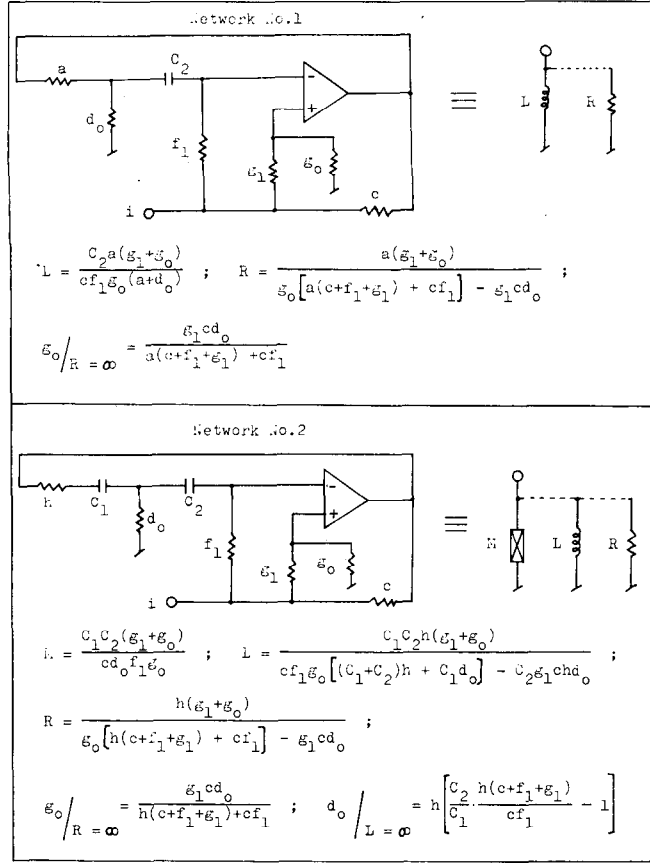
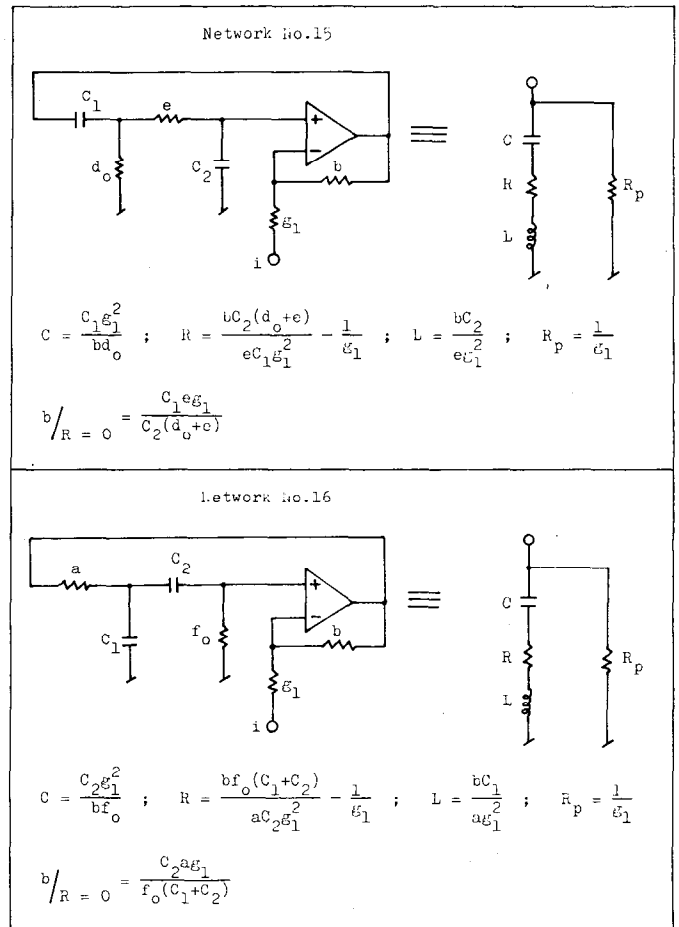
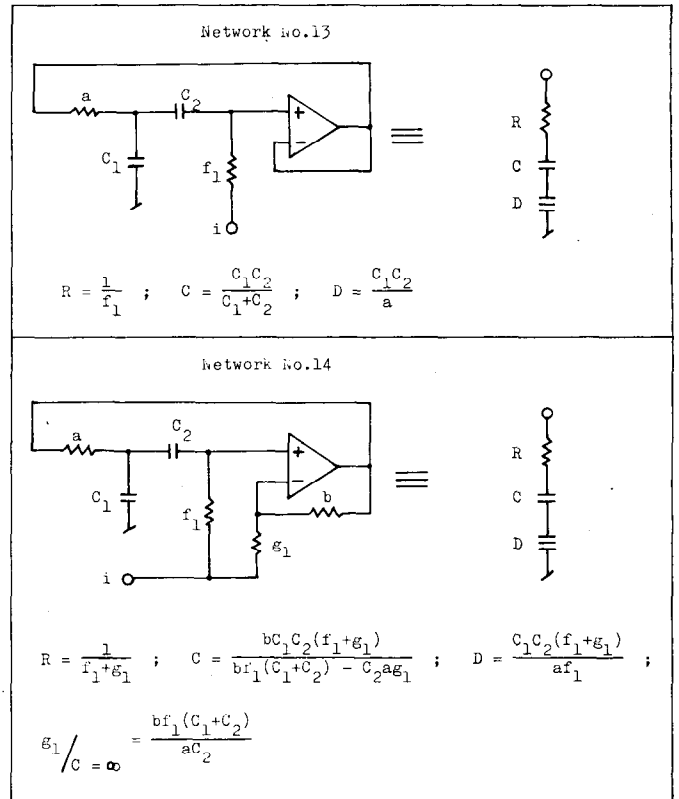
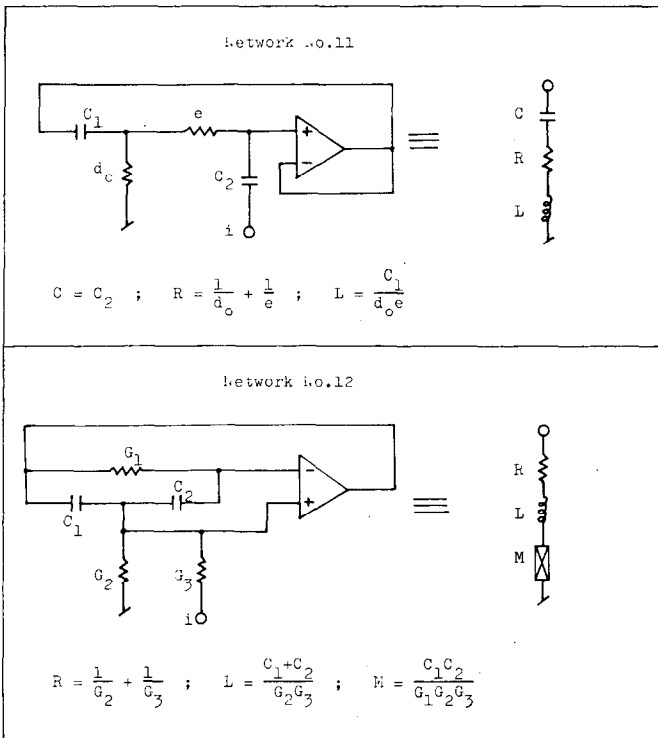
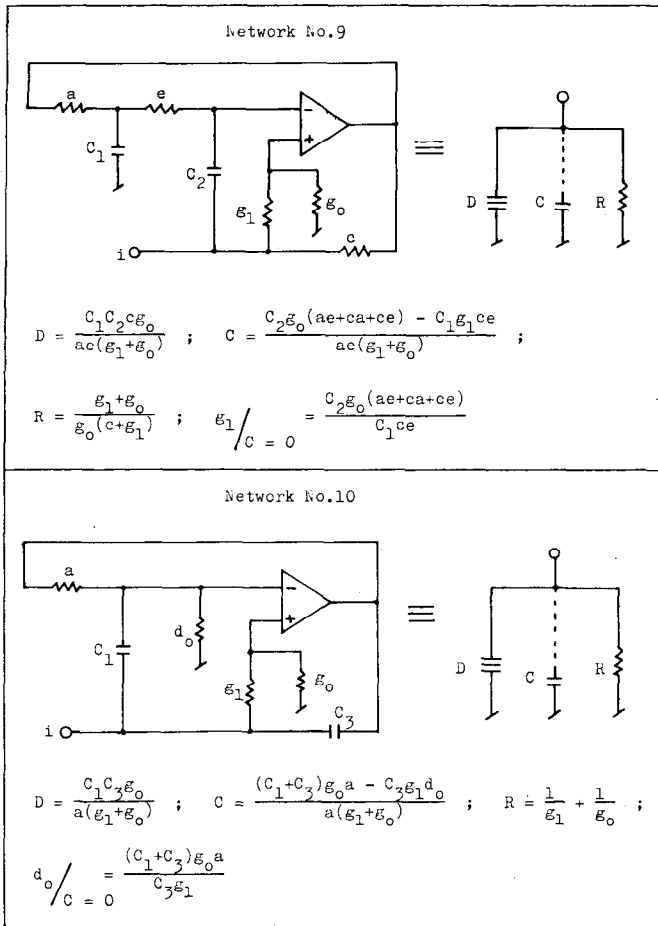


TABLE III (Continued)



may be readily obtained. Note that each of the networks is canonical in C .

It is interesting to note that networks 1–3 can be dimensioned such that they provide the components L (network 1), M (network 2), and D (network 3) by themselves. Thus these three networks are perhaps the most universal of the networks given in Table III, in that, among others, the six parallel and series impedance configurations of Table II can be obtained merely by adding the elements (i.e., E_1 and E_2 of Fig. 5) in parallel or series with the simulated element L , M , or D , respectively. It should be noted though, that the impedances thereby obtained are not necessarily canonical. For this reason some of the other networks may be preferable. In particular the series impedance configurations given as networks 11–16, which were obtained in a similar manner to networks 1–10, are generally canonical and more economical of components than series configurations obtained from networks 1–3. Networks 10 and 14 have been previously described in the literature ([16] and [10], respectively). Network 12 was obtained in a manner similar to the others, except that a different starting network topology (see Fig. 6(c)) was used. In this connection it should be pointed out that numerous additional impedance networks can be obtained by starting with other topologies than those used here. From there on the method follows the procedure outlined above. Naturally, each starting topology must be part of the fundamental topology represented by Fig. 1. In this regard, an obvious additional starting topology is the one shown in Fig. 6(c); it may be obtained from the topology of Fig. 6(b) by the complementary transformation [17].

In conclusion it may be useful to compare the method of driving-point impedance design described in this paper with the general method of driving-point impedance synthesis suggested by Sandberg [18]. Certainly, Sandberg's synthesis method is more general, in that any impedance function of arbitrary order can be synthesized with it. However the resulting network will generally not be canonical, nor will it necessarily have a low resistor count. Moreover, since it is to be expected that active impedance networks of order higher than two (or three) will depend as critically on the open-loop amplifier gain as is known to be the case for conventional active filters, it is doubtful whether single-opamp active driving-point impedances of order higher than two or three are practically feasible. By contrast, the impedance design suggested in this paper uses active networks that are compatible with well proven active filter building blocks and, like the latter, may readily be optimized for minimum passive component sensitivity and minimum gain-sensitivity product [14].

REFERENCES

- [1] H. J. Orchard, "Inductorless filters," *Electron. Lett.*, vol. 2, pp. 224–225, June 1966.
- [2] A. Antoniou, "New gyrator circuits obtained by using nullors," *Electron. Lett.*, vol. 4, pp. 87–88, Mar. 1968.
- [3] L. T. Bruton, "Frequency selectivity using positive impedance converter-type networks," *Proc. IEEE (Lett.)*, vol. 56, pp. 1378–1379, Aug. 1968.
- [4] L. T. Bruton, "Network transfer functions using the concept of frequency-dependent negative resistance," *IEEE Trans. Circuit Theory*, vol. CT-16, pp. 406–408, Aug. 1969.
- [5] L. T. Bruton and A. B. Haase, "Sensitivity of generalized immittance converter-embedded ladder structures," *IEEE Trans. Circuits Syst.*, vol. CAS-21, pp. 245–250, Mar. 1974.
- [6] K. Martin and A. S. Sedra, "Optimum design of active filters using the generalized immittance converter," *IEEE Trans. Circuits Syst.*, vol. CAS-24, pp. 495–503, Sept. 1977.
- [7] J. M. Rollett, "Economical RC Active Lossy Ladder Filters," *Electron. Lett.*, vol. 9, pp. 70–72, Feb. 1973.
- [8] H. J. Orchard and A. N. Willson, "New active-gyrator circuit," *Electron. Lett.*, vol. 10, pp. 261–262, June 1974.
- [9] F. Molo, "Parallel resonator with a resistance and a frequency-dependent negative resistance realized with a single operational amplifier," *IEEE Trans. Circuits Syst.*, vol. CAS-21, pp. 783–788, Nov. 1974.
- [10] R. H. Cheng and J. T. Lim, "Single opamp networks for shunt arms in ladder filters," in *Proc. Int. Symp. Circuits Syst.* Phoenix, AZ, pp. 313–316, Apr. 1977.
- [11] G. S. Moschytz, *Linear Integrated Networks: Fundamentals*. New York: Van Nostrand, 1974.
- [12] G. S. Moschytz and P. Horn, "The design of very-low-frequency (VLF) hybrid integrated networks using the morphological method," in *European Conf. Circuit Theory*, Genoa, Italy, pp. 515–522, Sept. 1976.
- [13] H. W. Bode, *Network Analysis and Feedback Amplifier Design*. New York: Van Nostrand, 1945.
- [14] G. S. Moschytz and P. Horn, "Reducing nonideal op-amp effects in active filters by minimizing the gain-sensitivity product (GSP)," *IEEE Trans. Circuits Syst.*, vol. CAS-24, pp. 437–445, Aug. 1977.
- [15] G. S. Moschytz, *Linear Integrated Networks: Design*. New York: Van Nostrand, 1975.
- [16] A. M. Soliman and S. S. Awad, "Canonical high-selectivity parallel resonator, using a single operational amplifier, and its applications in filters," *Electronic Circuits Syst.*, vol. 1, no. 4, pp. 145–148, July 1977.
- [17] G. S. Moschytz and P. Horn, "Optimising two commonly used active-filter building blocks using the complementary transformation," *Electronic Circuits Syst.*, vol. 1, no. 4, pp. 125–132, July 1977.
- [18] I. W. Sandberg, "Synthesis of driving-point impedance with active RC-networks," *Bell Syst. Tech. J.*, vol. 39, pp. 947–962, July 1960.
- [19] E. A. Guillemin, "Synthesis of Passive Networks." New York: Wiley, 1967.
- [20] C. A. Desoer and E. S. Kuh, *Basic Circuit Theory*. New York: McGraw-Hill, 1969.
- [21] P. Horn, "Contribution to the analysis, optimization and synthesis of active RC-Networks," Ph.D. thesis (in German), Swiss Federal Institute of Technology (ETH), Zürich, Switzerland, 1978.

+



Peter Horn (S'71–M'73) received the M.S. and Ph.D. degrees in electrical engineering from the Swiss Federal Institute of Technology, Zürich, Switzerland, in 1972 and 1978, respectively.

He is presently with the Institute of Telecommunications, Swiss Federal Institute of Technology.

+



George S. Moschytz (M'65–SM'76–F'78) received the M.S. and Ph.D. degrees in electrical engineering from the Swiss Federal Institute of Technology, Zürich, Switzerland, in 1958 and 1960, respectively.

From 1960 to 1962 he was with the RCA Laboratories Ltd., Zürich, Switzerland, where he worked on color TV signal transmission problems. In 1963 he joined Bell Telephone Laboratories, Inc. Holmdel, NJ, where as Supervisor of the Active Filter Group in the Data Commu-

cations Laboratory he investigated methods of synthesizing hybrid-

integrated linear and digital circuits for use in data transmission equipment. From 1972 to 1973 he was on a leave of absence from Bell Laboratories and Visiting Professor at the Swiss Federal Institute of Technology. Since 1973 he has been Professor of Electrical Engineering and Director of the Institute of Telecommunications at the Swiss Federal Institute of Technology. During the summer of 1977 he worked in the Transmission Networks Department at Bell Telephone Laboratories,

North Andover, MA. He is author of *Linear Integrated Networks: Fundamentals* (New York: Van Nostrand, 1974) and *Linear Integrated Networks: Design* (New York, Van Nostrand, 1975), has authored numerous papers in the field of active network theory, design and sensitivity, and holds several patents in these areas. His present interests are in the field of active and digital filters and signal processing.

Dr. Moschytz is a member of the Swiss Electrotechnical Society.

Noise and Sensitivity Optimization of a Single-Amplifier Biquad

HERBERT J. BÄCHLER, MEMBER, IEEE, WALTER GUGGENBÜHL, SENIOR MEMBER, IEEE

Abstract—Many papers have dealt either with noise or sensitivity optimization of second-order active networks. In this article a joint optimization criteria is developed for a well-known single-amplifier biquad (SAB). The noise performance and the sensitivity properties of the SAB are described by two free network parameters, namely the resistor ratio r^2 and the capacitor ratio c^2 . A two-dimensional object function is left to minimize for either low-noise or low-sensitivity design. Curves which determine the best r, c values are given for both design objectives. A comparison indicates that only a slight sacrifice of the overall sensitivity properties is required by the optimum noise design, while a significant increase in output noise can result if the circuit is designed for minimum sensitivities.

Several authors have dealt with the relationship between sensitivity and noise of active circuits [5]–[7]. From [6] it follows, that the same circuit structure once optimized for minimum sensitivities and once for minimum output noise brings out different results.

It is the purpose of this article to compare the sensitivity optimization and the noise optimization of second-order filters. Some general noise and sensitivity fundamentals are presented first and then applied to a single-amplifier biquad (SAB) circuit.

I. INTRODUCTION

THE NOISE properties of different RC-active filter structures have been analyzed by several authors [1]–[4]. A general noise analysis procedure, applicable to all single-amplifier second-order networks has been introduced in [2] and [4]. Depending on the application, different circuit design objectives have to be considered.

Second-order networks are very often used as basic building blocks to realize higher order networks. That application requires a large dynamic range.

Since the maximum output signal level is limited by the active element supply voltages, the dynamic range is optimized by minimizing the output noise level of the specific second-order blocks. Minimizing the total output noise power will therefore be the main circuit design directive in this paper.

II. GENERAL CIRCUIT DESCRIPTION

The following calculations are restricted to second-order networks using a single amplifier, according to Fig. 1(a). The circuit decomposes into a passive RC-4 terminal network and an active device with amplification K . The signal performance of the passive RC-network can be described by its short circuit admittance parameters. The active device contains an operational amplifier in the inverting mode with additional resistive, positive feedback. The operational amplifier (opamp) is assumed to be ideal with respect to the input and output resistances, the open loop gain is A , ($A \gg 1$).

With

$$t_{12} = \frac{-y_{21}}{y_{22}} \quad t_{32} = \frac{-y_{23}}{y_{22}} \quad (1)$$

the signal transfer function $T(s)$ from terminal 1 to the output yields

$$T(s) = \frac{K \cdot t_{12}(s)}{1 - K t_{32}(s)} = \frac{N(s)}{D(s)}, \quad s = j\omega. \quad (2)$$

Manuscript received December 28, 1977; revised July 13, 1978. This work was supported by the Hasler Foundation, Berne, Switzerland.

The authors are with the Department of Electronics, Swiss Federal Institute of Technology, Zurich, Switzerland.